Macroscopic biaxiality and electric-field–induced rotation of the minor director in the nematic

phase of a bent-core liquid crystal

Macroscopic biaxiality and electric-field–induced rotation of the minor director in the nematic phase of a bent-core liquid crystal

Mamatha Nagaraj[1], K. Merkel[1,2], J. K. Vij[1(a)] and A. Kocot[1,2(b)]

[1] *Department of Electronic and Electrical Engineering, Trinity College Dublin, University of Dublin*
Dublin 2, Ireland, EU
[2] *Institute of Physics, University of Silesia - Katowice, Poland, EU*

Abstract – Biaxiality in the nematic phase has been investigated for the bent-core liquid-crystal *para*-heptylbenzoate diester, using polarised IR spectroscopy. Anisotropic fluctuations of the nematic director are discussed in terms of the self-assembly of the chiral conformers. The ordering of the minor director for the homeotropicaly aligned sample is found to depend on the rubbing of the substrates of the cell and the amplitude of in-plane electric field. On increasing the in-plane electric field, the rotation of the minor director in the plane of the substrate is observed with an angle of approximately 45°, where initially the minor director is shown to lie along the rubbing direction. It is also shown that on the average the long axis of the molecules is normal to the substrate with surface treatment, with and without rubbing. The electric in-plane field combined with rubbing is shown to induce biaxial order in the nematic phase of a material with negative dielectic anisotropy for the first time.

Since the first prediction of biaxial nematic phase made by Freiser [1] and its discovery in lyotropic [2] and thermotropic [3–8] liquid crystals, the study of the biaxial nematic (N_b) phase has been interesting and physically challenging area of research in liquid-crystal physics. The use of biaxiality in changing the transmittance through the cell offers significant potential for increasing the speed of liquid-crystal displays. Simulation experiments on the bulk systems demonstrate that the short director in the N_b phase can effectively respond to the applied external field where the switching of the minor director is at least a factor of magnitude faster [8]. Despite such a prediction, biaxiality in the nematic phase has only been observed macroscopically in a few materials [9–11], the finding in some of these materials is still being strongly debated [8,12]. Results of the atomistic simulation of ODBP-Ph-C_7 system show that the biaxiality in the nematic phase in the bulk gets established [13], however the degree of biaxiality found so far is small because the local fluctuations are tending to reduce it. On the other hand, biaxiality arises naturally close to the external surface where the anchoring is strongly enforced [14]. Recently Dong *et al.* [15,16] determined the local order parameters S and D for the various benzene rings in the bent-core liquid crystalline molecular systems and they found that the conformation and ordering of the bent core significantly change between the uniaxial and biaxial nematic phases. Southern *et al.* [17] used Raman scattering to investigate biaxiality in the nematic phase of a bent-core material and determined the uniaxial and the biaxial order parameters for the first time for a biaxial nematic liquid crystalline phase. Recently Park *et al.* [18] determined these order parameters for another bent-core system and found that most order parameters show a second-order transition from the uniaxial to biaxial nematic phase. The importance of the alignment by surfaces and the external electric field have not been investigated in any detail before and these are being discussed here in terms of the orientational fluctuations of the minor director.

(a)E-mail: jvij@tcd.ie
(b)E-mail: akocot@mee.tcd.ie

ODBP-Ph-C7

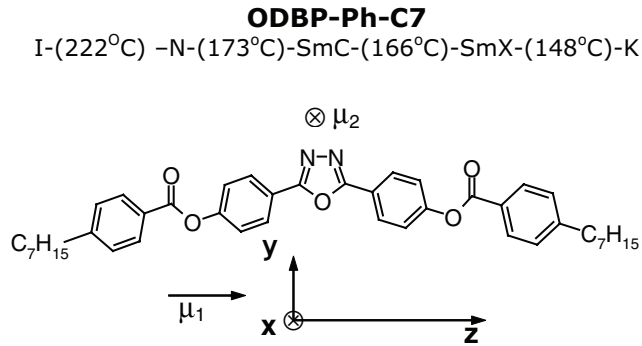I-(222°C) –N-(173°C)-SmC-(166°C)-SmX-(148°C)-K

Fig. 1: Molecular structure and the molecular frame of reference for ODBP-Ph-C_7.

This paper aims at investigating the macroscopic biax-iality and in advancing its physics by analysing the IR absorbance results for a bent-core nematic liquid-crystal *para*-heptylbenzoate diester (ODBP-Ph-C_7) [6], the structural formulae of which is given in fig. 1. The IR spectra for the homeotropic samples are recorded for different angles of polarization of the incident IR light. The effects of electric field and of rubbing the substrates of the cell are being examined. The results thus obtained are compared with those for the non-rubbed surfaces. In order to investigate the switching of liquid crystals with electric field, we develop a device configuration where the electrodes in the plane of the substrate are arranged at an angle of $\sim 45°$ to the rubbing direction. The surfaces are coated with a homeotropic alignment layer AL60702 (JSR Japan) and these are rubbed with different rubbing strengths (RS) [19]. Different values of RS are obtained (sample **b**: RS = 70 mm and sample **c**: RS = 90 mm) by altering the pile impression of the cloth in the rubbing machine and the results are compared with those of a non-rubbed cell (cell **a**).

The structure of the compound is simulated using the parallel quantum solution (PQS) package [20] (density functional theory (DFT) with Becke's hybrid three-parameter, Lee-Yang-Parr correlation functional, B3LYP). A standard Gaussian split-valence basis set with polarization and diffuse functions are used (6-31 + G*). Several conformers of the bent-core system are found with different orientations of each carbonyl dipoles with respect to the oxadiazol ring plane. The total permanent dipole moment of these conformers is found to range from 3.71 D to 7.1 D. An inverted rotation of the two ester linkages produces enantiomeric forms of a conformer. The corresponding IR frequencies are calculated using the PQS software and these are scaled using the scaled quantum mechanical (SQM) method [20]. The molecular long axis, z, is chosen to pass along the symmetrical ends of the core (the unit vector is assumed along the bow-string) and one of the perpendicular axes, y, is fixed along the C_2-axis of the core (arrow of the bow). Some of the vibrational modes are found to be the most promising features for studying the 3D orientational (both for the major and minor axes) ordering of the

ODBP-Ph-C_7 molecule. The bands used are: $1607 \, cm^{-1}$, $1491 \, cm^{-1}$ and $1157 \, cm^{-1}$, the transition dipole moments of these lie either along or make a small angle with the core of the mesogen. The transverse dipole modes which are also useful are: $1740 \, cm^{-1}$, $962 \, cm^{-1}$, $879 \, cm^{-1}$, $740 \, cm^{-1}$ and $699 \, cm^{-1}$. We choose only two bands for describing the orientational order of the system. These are: $\nu_1 = 1491 \, cm^{-1}$, *i.e.* the asymmetric stretching band of 2,5-bis (phenyl) - 1,3,4-oxadiazole and $\nu_2 = 740 \, cm^{-1}$, *i.e.* the out-of-plane deformation of the oxadiazole. These are chosen such that the polar and azimuthal angles for these bonds in the molecular frame are essentially inde-pendent of the conformations of the core. The carbonyl stretching $1740 \, cm^{-1}$ band is additionally used to analyse the rotation of the minor axis.

In order to probe the symmetry of the phase, we inves-tigate the dependence of IR absorbance on the angle of polarisation of the incident IR beam. The absorbance profiles *vs.* the angle of polarisation were analysed care-fully since a measurable deviation from the normal dispo-sition of the two absorbance profiles (observed for the orthorhombic, D_{2h}, symmetry) can in principle provide with a direct evidence of biaxiality [21] in this system. We did not observe any deviation from the orthorhombic symmetry (*i.e.* D_{2h} symmetry), see fig. 2(a), despite the observation of four-spots in the small-angle X-ray pattern that locally shows the skewed N phase [22]. Also measure-ments of the dependences of the absorbance components are made with respect the angle of oblique incidence for the two angles of polarisation: 0° and 90°. Both absorbance profiles (only one is shown here for convenience in fig. 2(a)) are found to be symmetrical with respect to those for the normal angle of incidence with an accuracy of better than 2°. This observation rules out the conjec-ture that the director may be tilted from the normal to the bounding plates. Figure 2(b) shows the tempera-ture dependences of the two perpendicular components of absorbance, A_X and A_Y for the $1491 \, cm^{-1}$ band measured in the plane of the homeotropic cells **a** and **c**. The labo-ratory coordinate system is chosen such that the X-axis coincides with the maximum of the absorbance for the $1491 \, cm^{-1}$ band. A difference between the two perpendic-ular components, A_X and A_Y, is a measure of the apparent biaxiality of the sample. A large drop in the absorbance for the $1491 \, cm^{-1}$ bands and a simultaneous increase in the absorbance for the $740 \, cm^{-1}$ band is observed both in the rubbed and unrubbed cells after the isotropic to nematic transition has occurred. This is a signature of the homeotropic alignment of the sample, fig. 2(b). For both samples, we can distinguish between the two regions of the nematic phase. At a temperature just below the isotropic-nematic transition, the measured absorbance is found not to depend on the angle of polarization as it is expected in uniaxial nematic phase. Absorbance becomes polariza-tion dependent 10 K below the $T_{I\text{-}N}$ temperature for the sample **a**, in the absence of substrate rubbing; a signa-ture of biaxial nematic phase. The uniaxial region shrinks to a temperature range of just 4 K for sample **c** when
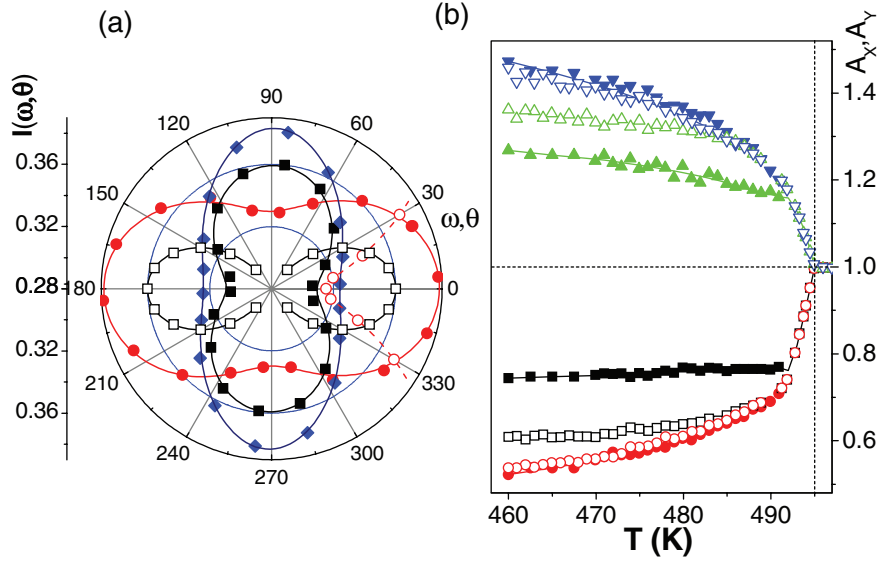
(a)

(b)

Fig. 2: (Colour on-line) Absorbance components for ODBP-Ph-C$_7$ sample measured in homeotropic alignment (cell thickness: $4\,\mu$m). (a) Polar plot for the absorbance peak intensity *vs.* i) angle of polarisation ω (filled symbols) and ii) *vs.* θ angle of oblique incidence (open symbols) at a temperature of 458 K and $E = 280$ V/mm : ●,○ for 1491 cm^{-1} band, (open circle data are multiplied by 0.8); ■,□ for 740 cm^{-1} and ◆ for 1718 cm^{-1} band. (b) Absorbances *vs.* temperature: ■,□ A_X, ●,○ A_Y for 1491 cm^{-1} band and ▲,△ A_X, ▼,▽ A_Y, for 740 cm^{-1} band: the open and solid symbols are for non-rubbed and weakly rubbed substrates (RS = 90 mm), respectively.

the substrates are rubbed. For non-rubbed substrates, the apparent biaxiality ($\Delta A = |A_X - A_Y|$) is finite but is rather low, however it shows a tendency to increase up to a value of 0.1 on decreasing the temperature. The measured values are easily reproducible and these are larger than the experimental errors. We find that the rubbing of substrates can increase the apparent biaxiality. The increase for the 1491 cm^{-1} band absorbance, A_X, in a rubbed cell, clearly indicates that the tilt fluctuations in the X-Z plane are becoming stronger than in Y-Z plane.

Two perpendicular components of the IR absorbance are expressed in terms of the scalar order parameters S, D, P, and C corresponding to the second-rank tensor order parameter and the orientation of the transition dipole, $\boldsymbol{\mu}$, in the molecular system. The parameters are defined by the three diagonal Saupe ordering matrices [7,23], one for each of the three axes, $i = X, Y, Z$; $S^i_{\alpha\beta} = \langle \frac{1}{2}(3l_{i,\alpha}l_{i,\beta} - \delta_{\alpha\beta})\rangle$. The scalar order parameters are expressed in terms of the elements of the Saupe matrix [24].

$$S = S^z_{zz}, \quad P = S^x_{zz} - S^y_{zz}, \quad D = S^z_{xx} - S^z_{yy}$$
$$\text{and} \quad C = (S^x_{xx} - S^x_{yy}) - (S^y_{xx} - S^y_{yy})]. \tag{1}$$

$$A_X/A_0 = 1 - (S - P)\left[(l_i)^2_n - \tfrac{1}{2}\left((l_i)^2_l + (l_i)^2_m\right)\right] \\ -\tfrac{1}{2}(D - C)\left((l_i)^2_l - (l_i)^2_m\right),$$
$$A_Y/A_0 = 1 - (S + P)\left[(l_i)^2_n - \tfrac{1}{2}\left((l_i)^2_l + (l_i)^2_m\right)\right] \\ -\tfrac{1}{2}(D + C)\left((l_i)^2_l - (l_i)^2_m\right), \tag{2}$$

$$(A_X + A_Y)/A_0 = 1 - S\left[(l_i)^2_n - \tfrac{1}{2}\left((l_i)^2_l + (l_i)^2_m\right)\right] \\ -\tfrac{1}{2}D((l_i)^2_l - (l_i)^2_m),$$
$$(A_X - A_Y)/A_0 = P\left[(l_i)^2_n - \tfrac{1}{2}\left((l_i)^2_l + (l_i)^2_m\right)\right] \\ -\tfrac{1}{2}C((l_i)^2_l - (l_i)^2_m). \tag{3}$$

Fig. 3: (Colour on-line) Order parameters for ODBP-Ph-C$_7$ samples with different surface anchorings: ▲,△ S, ■, □ D, ▼, ▽ P and ●,○ C: open and solid symbols are for non-rubbed and weak rubbed substrates (RS = 90 mm), respectively.

We choose only two bands: $\nu_1 = 1491$ cm^{-1} and $\nu_2 = 740$ cm^{-1} for calculating the orientational order parameters and their corresponding dipole moments $\boldsymbol{\mu}_1$ and $\boldsymbol{\mu}_2$ are parallel and perpendicular, respectively, to the molecular long axis of the mesogen core (fig. 1). Following the simulation of the molecular structure, we find that the polar angle is 0° for $\boldsymbol{\mu}_1$ and both polar and azimuthal angles for $\boldsymbol{\mu}_2$, are 90° and 14°, respectively.

Results for the two ODBP-Ph-C$_7$ samples with different boundary conditions are shown in fig. 3: **a** non-rubbed and **c** with a weak rubbing (RS = 90 mm). The estimated accuracy of the determined order parameters is better than 10% for S and P and 20% for D and C. The absorbance

components A_X and A_Y are related to A_0 in the above equation. A_0 is the mean absorbance. The latter could have been taken as found from measurements of the IR absorbance in the isotropic phase, close to the clearing temperature. However, A_0 is temperature dependent and is proportional to the dipole density, which increases with decreasing temperature. We devised a procedure for calculating A_0 for different temperatures [24]. The S parameter of the sample without rubbing is found to be rather low, nevertheless it turns out to be a typical value for the other banana systems found using NMR [16]. One of the possible explanations could have been that such a low-order parameter could have corresponded to the nematic director having been tilted with respect to the normal to the substrate. This may have resulted from the surface anchoring and from the skewed nematic domains arising from the cluster model following the observation of the X-ray pattern [22]. However, IR results clearly show that the molecules on the average are *not tilted* but are oriented normal to the substrate. These have tilt fluctuations stronger in the plane perpendicular to the rubbing direction (X-Z) than along the plane (Y-Z). This conjecture is further supported by results from the Raman scattering [17] for the order parameters $\langle P_{200} \rangle$, $\langle P_{220} \rangle$, $\langle P_{400} \rangle$ and $\langle P_{440} \rangle$, found for a compound C5-Ph-ODBP-Ph-OC12, with a structure similar to that reported here. For a tilted domain structure, we would have expected a negative value for $\langle P_{400} \rangle$; such a value may even have get more negative on increasing the tilt angle. But $\langle P_{400} \rangle$ is found to be positive and increases on lowering the temperature. It seems that the real reason for a rather low nematic order parameter is the prevalence of the strong anisotropic fluctuations as found by atomistic simulation [13]. This also well corresponds to the model of self-assembly given by Görtz and Goodby [25]. This model strongly suggests the formation of a ribbon spiralling locally around the axis which coincides with the C_2-axis of the core (bow director). The structure dynamically fluctuates and any external forces (*i.e.* those arising from homeotropic surface interactions) can suppress the helix formation. Rubbing the substrate, on the other hand, can promote the assembly of such a ribbon along this direction. The fluctuations of the long molecular axis would be stronger in the plane perpendicular to the rubbing direction (X-Z plane) than along the (Y-Z) plane as stated above. The model clearly reproduces the anisotropy in the molecular fluctuations observed in our experiment and leads to a rather low orientational order parameter.

The order parameter, D, a measure of the molecular biaxiality. A positive value of D was found, which means larger fluctuations of the x-axis (compared with y-axis) with reference to the Z-axis of the laboratory system. It is interesting to note a larger value of D is observed for a banana system than for a calamitic system. We find that the rubbing of the substrate practically does not influence the magnitude of the molecular biaxiality, D. The parameters P and C are the *extrinsic* and *intrinsic*

phase biaxialities, respectively, and these describe how the uniaxial and biaxial molecular properties contribute to the phase biaxiality [3]. A positive value of P indicates the average tilting of the molecules in the X-Z plane (*i.e.* perpendicular to the rubbing direction in the case of rubbed substrate, Y-axis). C is also positive which implies that the molecular x and y axes on the average are orientated closer to their corresponding X and Y axes of the laboratory system than *vice-versa* (*i.e.* Y and X). For the case of non-rubbed substrates of the cell, the determined value, the *intrinsic* biaxiality parameter is ~ 0.06; this is in agreement with NMR results ($\eta \sim 0.11$) [5]. Both parameters, P and C, significantly increase with rubbing strength. Such a behavior clearly demonstrates that both types of biaxialites (*extrinsic* and *intrinsic*) are enhanced by rubbing of the substrate. $\langle P_{200} \rangle$ and $\langle P_{220} \rangle$ describe the uniaxial and biaxial order parameters, respectively, and these are $S = \langle P_{200} \rangle \cong 0.75$, $P = \langle P_{220} \rangle \cong 0.1$ determined using Raman scattering for a similar compound C5-Ph-ODBP-Ph-OC12 [20]. These are larger compared with the S and P for ODBP-Ph-C$_7$ of our results using IR spectroscopy as well as found by Dong *et al.* [15] and Dong [16]. We surmise that S determined using Raman Scattering might be overestimated as the calculations are based on the assumption of the independent scattering occurring from each of the two arms of the molecule. The approximation is inherent in their assignment of the $1600\,\mathrm{cm}^{-1}$ dipoles parallel to each of the two arms of the mesogen core. Atomistic molecular dynamic simulations by Peláez and Wilson [13] also confirm the existence of a thermotropic biaxial phase in ODBF-Ph-C7. They show that the intermolecular associations originating from the large transverse dipole moment reinforce transverse orientational correlations driven by the steric interactions. The ferroelectric domains in the nematic phase are formed by a parallel association of the transverse oxadiazole dipoles. The simulation shows a destabilization of the ferroelectric domains and of the phase biaxiality on removal of the electrostatic interaction. Our results similarly show a competition between the orderings of the minor and the major directors. An increase in the orderings of the minor director is followed by a decrease in that for the major director (fig. 3).

In order to investigate the effect of the reorientation of the minor director by the electric field, two stripe electrodes ($2.5\,\mu\mathrm{m}$ thick and $2\,\mathrm{mm}$ wide) are placed in the plane of the substrate that make approximately an angle of $45°$ to the rubbing direction. The gap between the electrodes is fixed as $840\,\mu\mathrm{m}$ (cell **b**: RS $= 70\,\mathrm{mm}$). The in-plane switching of the bent-core mesogen observed under polarising optical microscope is shown in fig. 4 (the rubbing makes an angle of $\sim 40°$ to the edges of the electrodes in this particular cell). In the absence of electric field, when the rubbing direction coincides with the polariser direction, the field of view is dark and it turns bright when the rubbing direction makes an angle of $\sim 45°$ to the polariser (fig. 4(a) and (b)). But when
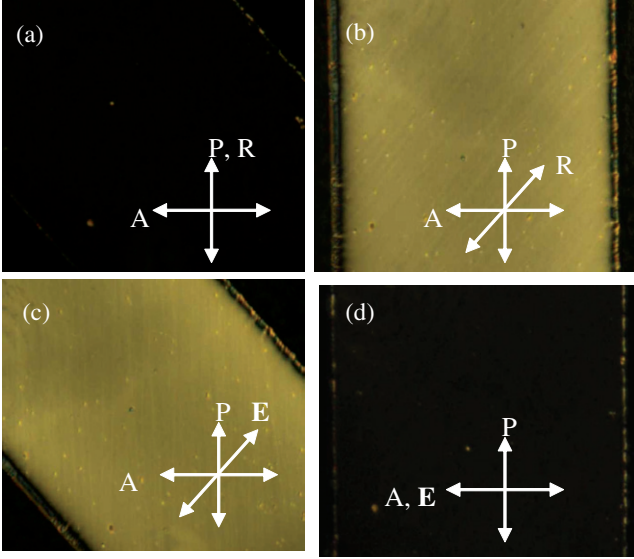
Fig. 4: (Colour on-line) Textures from a $4\,\mu m$ rubbed homeotropic cell for a temperature of 450 K. P = Polariser, A = Analyser and R = Rubbing, $\mathbf{E}$ = electric-field direction. (a), (b) are recorded before applying the electric field for the two positions of the sample holder ($0°$ and $\sim 50°$) with respect to P and A. (c) and (d) are for $U/d = 0.7\,\mathrm{V}/\mu m$, frequency 1 kHz. The axis of the strongest fluctuations of the nematic director is along A in (a) (at $E = 0$) and then along P, in (d) (for $E > E_{\mathrm{saturation}}$). Electrodes are made up of aluminium foils.

a sufficient large electric field is applied, due to the in-plane switching (alignment of the electric dipole moment along the field direction), the situation reverses (fig. 4(c) and (d)). Figure 5(b) shows the view of the cell in the $(X\text{-}Y)$ plane of the substrate. Any rotation of the molecules by the electric field can be observed through a shift in the IR absorbance profile $vs.$ the angle of polarisation, fig. 5(a). In particular, the absorbance profiles for the bands $740\,\mathrm{cm}^{-1}$, $879\,\mathrm{cm}^{-1}$, $1740\,\mathrm{cm}^{-1}$ provide a direct insight into the distribution of the molecular short axes since the corresponding transition dipoles are lateral to the long molecular axis. The position of the maximum of absorbance at a particular field indicates the favourable orientation of the corresponding transition dipole moment. On the other hand, the absorbance profile of a longitudinal dipole yields information about the projection of the long molecular axis onto the $(X\text{-}Y)$ plane thus reflecting the evolution of the distribution of the long axes. We applied a square wave signal of frequency 1 kHz and the amplitude is varied up to 400 V across the gap of the electrodes. On increasing voltage across the gap, we observe a gradual shift in the absorbance maximum for the lateral dipoles ($740\,\mathrm{cm}^{-1}$ band and $1740\,\mathrm{cm}^{-1}$), from the rubbing direction towards the direction of the electric field, fig. 5(d), (e). A similar shift is observed for the $1491\,\mathrm{cm}^{-1}$ band, but the maximum is shifted by $90°$ with respect to that for the lateral dipole moments.

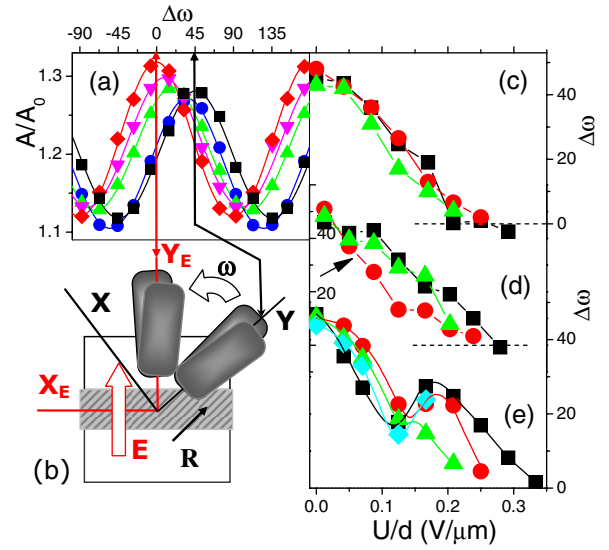Additionally the external electric field influences the orientational ordering of the sample as shown by the

Fig. 5: (Colour on-line) (a) Evolution of the absorbance profile $740\,\mathrm{CM}^{-1}$ $vs.$ polarizer angle following an application of the electric field of amplitudes varying between 0 V ($\blacksquare$) and $2\,\mathrm{V}/\mu m$ ($\blacklozenge$). (b) View of the cell in the substrate plane ($X\text{-}Y$). Rotation angles of the absorbance maximum $vs.$ amplitude for 1 kHz square wave voltage: (c) for $1491\,\mathrm{cm}^{-1}$ band, (d) for $1740\,\mathrm{cm}^{-1}$ band and (e) for $740\,\mathrm{cm}^{-1}$ at temperatures: $\blacksquare$ 458 K, $\bullet$ 468 K, $\blacktriangle$ 478 K and $\blacklozenge$ 488 K.
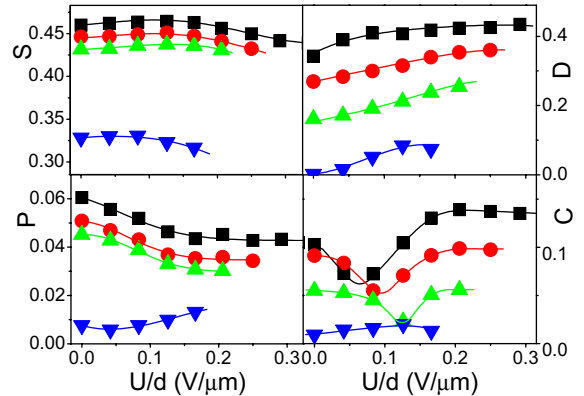

Fig. 6: (Colour on-line) Order parameters: S, D, P and C $vs.$ electric field for the sample with weakly rubbed substrates of the rubbing strength (RS = 70 mm) for different temperatures: $\blacksquare$ 458 K, $\bullet$ 468 K, $\blacktriangle$ 478 K and $\blacktriangledown$ 488 K.

field dependencies of the order parameters, fig. 6. The clearest observation is that of an increase in the molecular biaxiality, D, by increasing the electric field. Two of the phase biaxiality parameters, P and C, behave differently. For the biaxial nematic phase, the $extrinsic$ biaxiality, P, decreases significantly with the field up to a threshold value and then it saturates to the level of $\sim 25\%$ below the initial value, whereas the $intrinsic$ biaxiality, C, initially decreases by a factor of 2 and then it increases to a value higher than its initial value. It seems that the minor director does not rotate uniformly with increase in the electric field. For rather weak fields it is possible that the

torque may not be strong enough to completely rotate the minor director to the equilibrium position in the time duration of the half-period of the field. When the field is above $0.2\,\mathrm{V}/\mu$m the maxima of the angular profile for the $740\,\mathrm{cm}^{-1}$ band rotates by an angle of $\sim 45°$, the electric field then takes entire control of the alignment of the major and minor directors. Since the ODBP-Ph-C$_7$ material has negative dielectric anisotropy, one can expect a significant rise in the homeotropic order with increasing electric field. This is confirmed both by an initial increase in S and a decrease in the P parameter with the field. For the case of uniaxial nematic phase at a temperature of $488\,\mathrm{K}$, the field-induced behaviour in this system is clearly different since the biaxial order as the main origin of the electric torque is missing at low fields at least. At higher fields, however, the field-induced transition to biaxial phase possibly occurs. This transition significantly increases the biaxial order parameters, D, P and C.

One of the possible ways of examining the alignment of the minor director by surfaces and the external electric field is to examine the orientational fluctuations. Due to the low elastic constant involved in the rotation of the minor director, the fluctuations are large enough and these tend to destroy the spontaneous long-range alignment of the minor director. This is one of the possible reasons as to why the thermotropic biaxial nematic phase is not commonly observed experimentally. It seems that the nematic phase has local biaxial and polar orderings due to the cooperative alignment of the short axes and those of the electric dipoles. In the absence of electric field or/and other aligning forces (*i.e.* rubbing), the alignment of the minor director may be destroyed. It seems that rubbing of the substrates modifies the distribution of the minor axes of the molecules. The non-polar nematic is converted into a polar nematic on applying **E** greater than the threshold. The minor director is aligned at least locally with its dipole moments parallel to the applied field over a macroscopic volume. A net bulk polarization is then induced and its direction can be reversed by changing the sign of **E**. On the other hand, the macroscopic order of the minor director once established (at a particular amplitude of **E**) is not altered under the field reversal. The molecular biaxiality, D, increases on the application of the electric field and so does the polar order of the molecular dipoles and the biaxial order of the short axis. Thus an increase in the *intrinsic* biaxial order parameter, C, arises mostly from an increase in the molecular biaxiality, D. An increase in temperature destroys both kinds of orderings due to an increase in the molecular mobility.

$* * *$

REFERENCES

[1] FREISER M., *Phys. Rev. Lett.*, **24** (1970) 1041.
[2] YU L. J. and SAUPE A., *Phys. Rev. Lett.*, **45** (1980) 1000.
[3] ACHARYA B., PRIMARK R. A., DINGEMANS T. J., SAMULSKI E. T. and KUMAR S., *Pramana*, **61** (2003) 231.
[4] SEVERING K. and SAALWACHTER K., *Phys. Rev. Lett.*, **92** (2004) 125501.
[5] MADSEN L. A., DINGEMANS T. J., NAKATA M. and SAMULSKI E. T., *Phys. Rev. Lett.*, **92** (2004) 145505.
[6] ACHARYA B. R., PRIMAK A. and KUMAR S., *Phys. Rev. Lett.*, **92** (2004) 145506.
[7] MERKEL K., KOCOT A., VIJ J. K., KORLACKI R., MEYER T. and MEHL G. H., *Phys. Rev. Lett.*, **93** (2004) 237801.
[8] FRANCESCANGELI O., STANIC V., TORGOVA S. I., STRIGAZZI A., SCARAMUZZA N., FERRERO C., DOLBNYA I. P., WEISS T. M., BERARDI R., MUCCIOLI L., ORLANDI S. and ZANNONI C., *Adv. Funct. Mater.*, **19** (2009) 2592.
[9] LEE J.-H., LIM T.-K., KIM W.-T. and JIN-II J., *J. Appl. Phys.*, **101** (2007) 034105.
[10] LEE G. S., CHO J. S., KIM J. C., YOON J.-H and SHIN S. T., *J. Appl. Phys.*, **105** (2009) 094509.
[11] YOU J., JUNG J. Y., RHIE K., PERGAMENSHCHIK V. M. and SHIN S. T., *J. Korean Phys. Soc.*, **52** (2008) 342.
[12] STANNARIUS R., *J. Appl. Phys.*, **104** (2008) 036104.
[13] PELÁEZ J. and WILSON M., *Phys. Rev. Lett.*, **97** (2006) 2157801.
[14] BISCARI P., NAPOLI G. and TURZI S., *Phys. Rev. E*, **74** (2006) 031708.
[15] DONG Y. R., KUMAR S., PRASAD V. and ZHANG J., *Chem. Phys. Lett.*, **448** (2007) 54.
[16] DONG R. Y., *J. Phys. Chem. B*, **113** (2009) 1933.
[17] SOUTHERN C. D., BRIMICOMBE P. D., SIEMIANOWSKI S. D., JARADAT S., ROBERTS N., GÖRTZ V., GOODBY J. W. and GLEESON H. F., *EPL*, **82** (2008) 56001.
[18] PARK M. S., YOON B.-J, PARK J. O., PRASAD V., KUMAR S. and SRINIVASARAO M., *Phys. Rev. Lett*, **105** (2010) 027801.
[19] PARK S.-H., *J. Ind. Eng. Chem.*, **7** (2001) 316; HASEGAWA M., in *Alignment Technologies and Applications of Liquid Crystal Devices*, edited by TAKATOH K., HASEGAWA M., KODEN M., ITOH N., HASEGAWA R. and SAKAMOTO M. (Taylor & Francis, Oxford) 2005, Chapt. 2, p. 27.
[20] PULAY P., BAKER J. and WOLINSKI K., *Parallel Quantum Solutions*, http://www.pqs-chem.com .
[21] KARAHALIOU P. K., VANAKARAS A. G. and PHOTINOS D. J., *J. Chem. Phys.*, **131** (2009) 124516.
[22] FRANCESCANGELI O. and SAMULSKI E. T., *Soft Matter*, **6** (2010) 2413; SAMULSKI E. T., *Liq. Cryst.*, **37** (2010) 669.
[23] DUNMORE D. and TORIYAMA H., in *Handbook of Liquid Crystals*, edited by DEMUS D., GOODBY J., GRAY G. W., SPIESS H.-W. and VILL V., Vol. **1** (Weinheim Wiley-VCH), 1998, Chapt. VII.1, p. 189.
[24] KOCOT A. and VIJ J. K., *Liq. Cryst.*, **37** (2010) 653.
[25] GÖRTZ V. and GOODBY J., *Chem. Commun.*, **26** (2005) 3262; GÖRTZ V., SOUTHERN C., ROBERTS N. V., GLEESON H. F. and GOODBY J. W., *Soft Matter*, **5** (2009) 463.